

Supplementary Material for
**Water droplet attraction and coalescence on
liquid-crystal-infused textured and porous surfaces**

Filip Ferš^a, Xiaoguang Wang^{b,c}, and Uroš Tkalec^{a,d,e*}

^aInstitute of Biophysics, Faculty of Medicine, University of Ljubljana, 1000 Ljubljana, Slovenia

^bWilliam G. Lowrie Department of Chemical and Biomolecular Engineering, The Ohio State University, Columbus, OH 43210, U.S.A.

^cSustainability Institute, The Ohio State University, Columbus, OH 43210, U.S.A.

^dFaculty of Natural Sciences and Mathematics, University of Maribor, 2000 Maribor, Slovenia

^eDepartment of Condensed Matter Physics, Jožef Stefan Institute, 1000 Ljubljana, Slovenia

*Corresponding author: uros.tkalec@mf.uni-lj.si

White light interferometry

To determine the thin film thickness on LCITS obtained by spin-coating, we used white light interferometry. The experimental setup is shown in Fig. S1a. The reflectance spectra of light reflected from the silicon micropillars infused with 5CB in the isotropic phase were measured using a reflection probe (Fig. S1b), which was connected to a spectrometer (AvaSpec-ULS2048CL-EVO, Avantes) and a light source (AvaLight-Cal-Mini, Avantes) (Fig. S1c). The probe was mounted on an adjustable stage and moved vertically. For calibration a white reflectance standard was used. The reflectance is calculated as:

$$R(\lambda) = \frac{I(\lambda) - B(\lambda)}{I_{\text{ref}}(\lambda) - B(\lambda)}, \quad (\text{S1})$$

where $I(\lambda)$ is the measured light intensity, $B(\lambda)$ is the background measurement taken with the shutter closed, λ is the wavelength of light, and $I_{\text{ref}}(\lambda)$ is the reference measurement from the white standard.

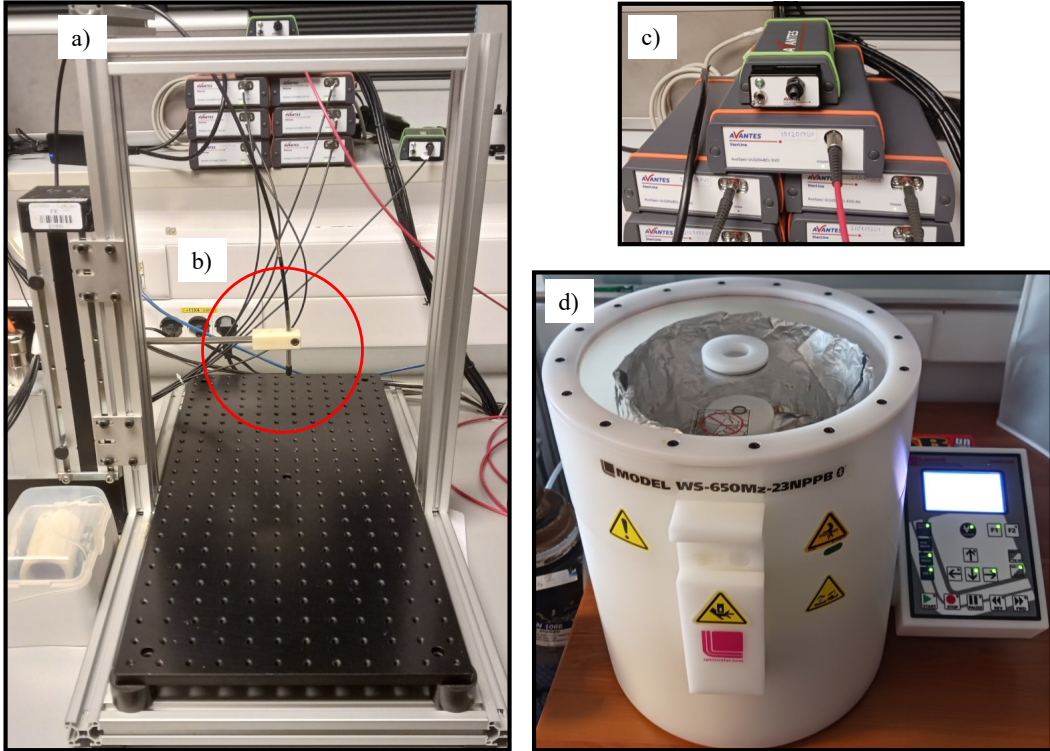


Figure S1: Experimental setup for white light interferometry. a) Overview of the complete experimental setup. b) Reflection probe (highlighted with a red circle) mounted on a computer-controlled, vertically adjustable stage. c) Light source and spectrometer used for thin film thickness measurements. d) Spin-coater used in experiments.

The reflectance of a thin film of thickness b and refractive index n_2 for a linearly polarized ray with electric field amplitude E_0 at normal incidence can be expressed in terms of the amplitude reflection coefficients as:

$$R(\lambda) = \left| \frac{r_{A,LC} + r_{LC,S} e^{i\phi}}{1 + r_{A,LC} r_{LC,S} e^{i\phi}} \right|^2 = \frac{r_{A,LC}^2 + r_{LC,S}^2 + 2r_{A,LC} r_{LC,S} \cos\left(\frac{4\pi n_{LC} b}{\lambda}\right)}{1 + r_{A,LC}^2 r_{LC,S}^2 + 2r_{A,LC} r_{LC,S} \cos\left(\frac{4\pi n_{LC} b}{\lambda}\right)}, \quad (\text{S2})$$

where $\phi = 4\pi n_2 b / \lambda$, $r_{A,LC}$ is the amplitude reflection coefficient at the air-liquid crystal interface, $r_{LC,S}$ is the amplitude reflection coefficient at the LC-substrate interface, and n_{LC} is the refractive index of the LC. Since $r_{A,LC}^2 \ll 1$, where $r_{A,LC} \approx 0.044$ for $n_{LC} = 1.5357$, Eq. (S2) simplifies to:

$$R(\lambda) \approx r_{LC,S}^2 + 2r_{A,LC} r_{LC,S} \cos\left(\frac{4\pi n_{LC} b}{\lambda}\right). \quad (\text{S3})$$

Because $r_{A,LC}$ and $r_{LC,S}$ vary slowly with wavelength, they can be treated as constants A_1 and A_2 , further simplifying Eq. (S3) to:

$$R(\lambda) \approx A_1 + A_2 \cos\left(\frac{4\pi n_{LC} b}{\lambda}\right). \quad (\text{S4})$$

To determine the thickness of the thin LC film, we first represent the measured reflectance spectrum in k -space and obtain $R(k)$. Next, a second-order polynomial $T(k)$ is subtracted from the spectrum to obtain $\tilde{R}(k) = R(k) - T(k)$, which removes the slowly varying contribution arising from the wavelength dependence of A_1 and A_2 . Finally, we compute the discrete Fourier transform of $\tilde{R}(k)$ and fit a Cauchy distribution to the peaks of the spectrum. The Cauchy distribution is given by:

$$f(x) = \frac{C\gamma}{\pi[\gamma^2 + (x - x_0)^2]}, \quad (\text{S5})$$

where C is the peak amplitude, γ is the peak width, and x_0 is the position of the peak on the x -axis. All three parameters are fitting parameters. In our case, the peak positions correspond to the mean value $2n_{\text{LC}}b$, from which we can calculate the thickness b of the thin film, where n_{LC} is taken as the average value $n_{\text{LC}} = 1.5357$, which in principle depends on the wavelength. Fig. S2 shows one of the thin film thickness measurements. Because the micropillars are completely submerged, reflection of light from the top of the pillars and the bottom between the pillars produces interference, which appears in the reflectance spectrum as a superposition of cosine components. As a result, the Fourier transform of $\tilde{R}(k)$ has a bimodal distribution, which in Fig. S2 appears as two peaks with relative intensities dependent on the fraction of the micropillar area.

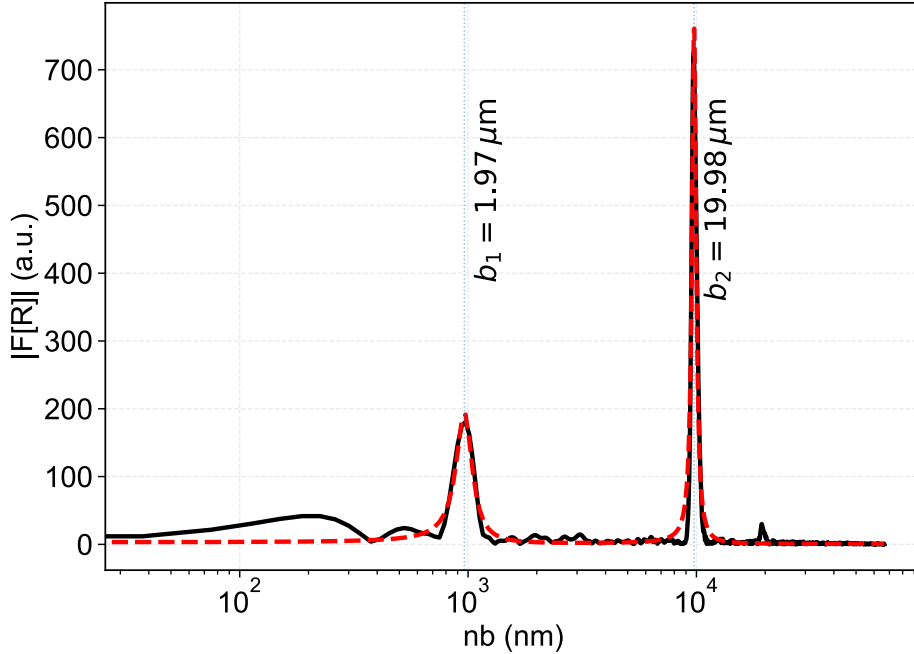


Figure S2: A thin film measurement obtained by white light interferometry. Shown is the Fourier amplitude spectrum $R(k)$ calculated from the measured reflectance. Two distinct peaks are visible, each fitted with a Cauchy distribution. Their positions on the x -axis correspond to the local film thickness. The first peak position corresponds to the smaller thickness $b_1 \approx 2 \mu\text{m}$ and arises from reflections at the LC-micropillar tops layer, while the second peak position corresponds to the larger thickness $b_2 \approx 20 \mu\text{m}$, which arises from reflections at the LC-substrate layer. The pillar height can therefore be obtained as the difference $b_2 - b_1 = 17 \pm 0.5 \mu\text{m}$.

Spin-coating

As described in Section 2.2 of the main text, excess 5CB was drop-cast onto a clean substrate and spin-coated at approximately 500 rpm using a gradual acceleration profile to achieve a uniform LC layer with a thickness of about $20 \mu\text{m}$. The spin-coater is shown in Fig. S1d. To determine the required rotation speed, we first performed a calibration procedure using the same controlled drop-cast volume and identical acceleration setting at different rotation speeds. After spin-coating for 60 s, the sample was heated into the isotropic phase and the resulting film thickness was measured using white light interferometry. The measured film thickness as a function of rotation speed (rpm) is shown in Fig. S3. From this calibration, we selected 500 rpm as the rotation speed, ensuring that the microstructured surface was fully infused while maintaining a stable, uniform thin film above the micropillar array.

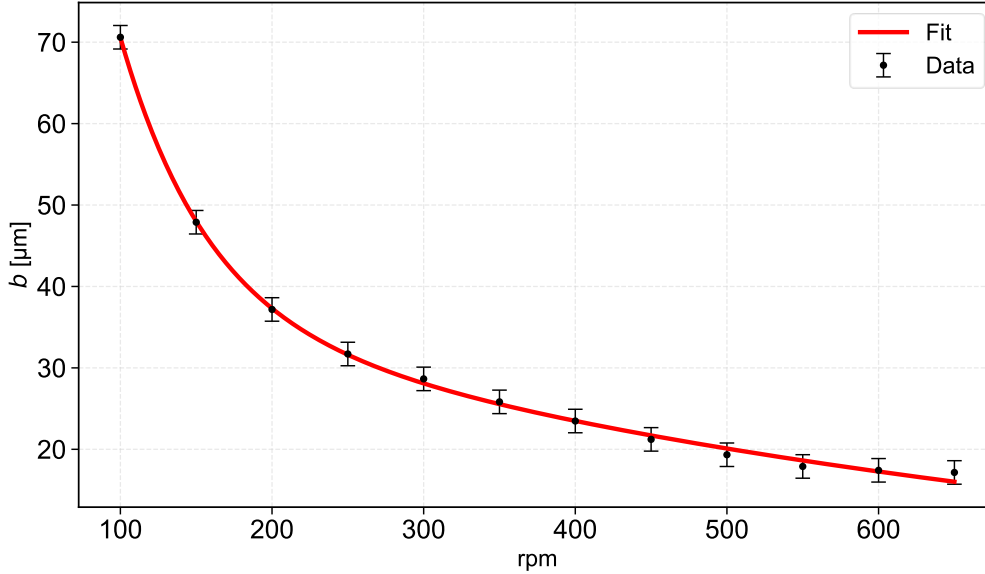


Figure S3: Measured LC film thickness b_2 as a function of spin-coater rotation speed (rpm). Data points represent the mean film thickness of multiple measurements at each rpm, and the error bars indicate the standard deviation over 5 independent measurements per rpm. The data were fitted with an exponential decay function.

Parameter values used in calculations

Here we list additional parameter values, used in calculations but omitted from the main text.

LC	Phase	T [$^{\circ}\text{C}$]	ρ [kg/m^3]	η_i [mPas]
5CB	N	30	1013	$\eta_1 = 77, \eta_2 = 20, \eta_3 = 32$
	I	40	1006	$\eta_I = 21$
8CB	N	40	979	$\eta_1 = 40, \eta_2 = 25, \eta_3 = 30$
	I	50	970	$\eta_I = 20$
Water	Liquid	30	996	0.80
		40	992	0.66
		50	988	0.55

Table S1: Densities (ρ) of 5CB and 8CB in the nematic (N) and isotropic (I) phases^{1,2}, and of water³ at the corresponding temperatures (T), as well as viscosity coefficients (η_i)^{4,5} of all the liquids, are given. In the isotropic phase, the viscosity coefficients of the LCs become identical and reduce to a single shear viscosity (η_I).

References

- [1] M. Sandmann, F. Hamann and A. Würflinger, *Z. Naturforsch. A*, 1997, **52**, 739–747.
- [2] M. Sandmann and A. Würflinger, *Z. Naturforsch. A*, 1998, **53**, 787–792.
- [3] W. Wagner and A. Pruß, *J. Phys. Chem. Ref. Data*, 2002, **31**, 387–535.
- [4] K. Mukai, F. Kishi and T. Amari, *Nihon Reoroji Gakk.*, 1997, **25**, 155–160.
- [5] A. G. Chmielewski, *Mol. Cryst. Liq. Cryst.*, 1986, **132**, 339–352.

Videos

Video S1

Capillary-assisted droplet attraction (Stage I) on LCIPS. The capillary-driven droplet-droplet interaction was recorded at 10000 fps in the nematic phase (top) and 5000 fps in the isotropic phase (bottom). In the example shown, the droplet radii are $R = 0.5$ mm. The LC film thickness on LCIPS was approximately 100 μm . See the **Experimental details** section of the main text for material properties. The captured videos shown are slowed down by a factor of 13.

Video S2

Capillary-assisted droplet attraction (Stage I) on LCITS. The capillary-driven droplet-droplet interaction was recorded at 5000 fps in the nematic phase (top) and 10000 fps in the isotropic phase (bottom). In the example shown, the droplet radii are $R = 0.35$ mm (top) and $R = 0.49$ mm (bottom). The LC film thickness on LCITS was approximately 20 μm , including the height of the micropillars. See the **Experimental details** section of the main text for material properties. The video is slowed down by a factor of 71 (top) and 250 (bottom).

Video S3

Droplet merging (Stage III) on LCIPS. Droplet merging was recorded at 10000 fps. The video shows droplet merging on LCIPS in the nematic phase (top) and isotropic phase (bottom). In the example shown, the droplet radii are $R = 0.51$ mm (nematic) and $R = 0.34$ mm (isotropic). The merging process is slowed down by a factor of 333 (top) and 416 (bottom). See the **Experimental details** section of the main text for material properties.

Video S4

Droplet merging (Stage III) on LCITS. Droplet merging was recorded at 10000 fps. The video shows droplet merging on LCITS in the nematic phase (top) and isotropic phase (bottom). In the example shown, the droplet radii are $R = 0.35$ mm (top) and $R = 0.49$ mm (bottom). The merging process is slowed down by a factor of 500. See the **Experimental details** section of the main text for material properties.